Raman Spectroscopic and X-ray Diffraction Studies on Concentrated Aqueous Zinc(II) Bromide Solution at High Temperatures

Toshiyuki Takamuku*, Mikito Ihara, Toshio Yamaguchi, and Hisanobu Wakita

Department of Chemistry, Faculty of Science, Fukuoka University, Nanakuma, Jonan-ku, Fukuoka 814-01, Japan

Z. Naturforsch. **47a**, 485–492 (1992); received November 27, 1991

Raman and X-ray scattering experiments have been performed on an aqueous zinc(II) bromide solution with molar ratio $[H_2O]/[ZnBr_2]=10$ at 25 to 140 °C. The intensity of the totally symmetric Zn–Br stretching vibration (ν_1) for the dibromozinc(II) complex increased with increasing temperature while that for the tetrabromo complex decreased. A broad band assigned to the symmetric Zn–O stretching vibration (ν_1) for the aqua zinc(II) ion decreased in intensity with increasing temperature. The X-ray diffraction data revealed that the average number of the Zn–Br interactions within the zinc(II) bromo complexes does not change with temperature, whereas the number of Br ··· Br nonbonding interactions within the complexes decreases from 1.8 at 25 °C to 1.5 at 100 °C. From both Raman and X-ray data it is concluded that with increasing temperature the dibromo species is favored, whereas the tetrabromo and aqua zinc(II) species are unstable in the solution. The analysis of the X-ray diffraction data has shown that the mean Zn–Br bond length within the zinc(II) bromo complexes shortens gradually with increasing temperature, accompanied with an increase in the interligand Br ··· Br distance. This finding suggests that the Br–Zn–Br bond angle increases with decreasing Zn–Br distance for the lower zinc(II) bromo complexes. The equilibrium shift of the zinc(II) bromo complexes with temperature is discussed on the basis of ion-ion, ion-water, and water-water interactions.

Key words: Raman spectroscopy, X-ray diffraction, Zinc(II)bromide, High temperature, Solution structure

1. Introduction

Structural investigations on solutions at the atomic scale in a wide range of temperature and pressure are essential in understanding the physico-chemical properties of, and chemical reactions in the solutions. Also, information about the properties of solutions under extreme conditions is needed in the fields of chemical synthesis and geochemistry. Such studies, however, are scarce because of experimental difficulties [1–6].

Aqueous solutions of zinc(II) halides have extensively been investigated at ambient temperature and pressure by various techniques [7–21]. Shchukarev et al. [11] and Gerding [12] have determined the thermodynamic parameters of stepwise complex formation between zinc(II) and halide ions (Cl^-, Br^-, and I^-). Wertz and Bell [13] performed X-ray diffraction measurements on aqueous zinc(II) chloride and reported that the pseudotetrahedral complex, $[ZnCl_2(OH_2)_2]$, is mainly formed in the solution. According to an X-ray and Raman scattering study on aqueous solutions $ZnCl_2 \cdot RH_2O$ ($R=[H_2O]/[ZnCl_2]$) by Yamaguchi et al. [14], tetrahedral complexes $[ZnCl_n(OH_2)_{4-n}]^{(2-n)+}$ are predominantly formed and the average number of Zn–Cl interactions increases from 2.4 for R = 6.2 to 3.4 for R = 1.8. Johansson et al. determined the structures of individual zinc(II) bromo [15] and iodo [16] complexes in aqueous zinc(II) halide solutions from X-ray diffraction measurements combined with Raman and IR spectra. All the Raman spectral measurements on aqueous zinc(II) halides solutions [17–21] have suggested that the $[ZnX_n(OH_2)_{4-n}]^{(2-n)+}$ complexes (X^- = halide ion) are formed.

At lower temperatures, Kanno and Hiraishi [22] made a Raman spectroscopic investigation on glassy aqueous zinc(II) halide solutions vitrified at liquid nitrogen temperature and have concluded that the tetrahalogeno complex, $[ZnX_4]^{2-}$ (X^- = Cl, Br, and I),

* On leave from Aqua Laboratory, Research and Development Division, TOTO Ltd., Nakashima, Kokurakita-ku, Kitakyushu 802, Japan.

Reprint requests to Prof. T. Yamaguchi, Department of Chemistry, Faculty of Science, Fukuoka University, Nanakuma, Jonan-ku, Fukuoka 814-01, Japan.

0932-0784 / 92 / 0300-0485 $ 01.30/0. – Please order a reprint rather than making your own copy.

and the octahedral aqua zinc(II) ion, $[Zn(OH_2)_6]^{2+}$, are preferentially formed in the glassy solutions, while the dihalogeno complex, $[ZnX_2(OH_2)_2]$, is unstable. Recently, we have performed Raman and X-ray scattering measurements on supercooled and glassy aqueous zinc(II) iodide [23] and bromide [24] solutions and have found that in the supercooled state as well as in the glassy state the amount of the tetrahalogeno and the aqua zinc(II) species increases gradually with decreasing temperature while the dihalogeno species diminishes with temperature for both bromide and iodide solutions. In addition, it has been found that the tribromozinc(II) complex is also unstable in the aqueous bromide solutions at the low temperatures, in contrast with the stable triiodo species in the corresponding iodide solutions. On the basis of these findings we have proposed that the following equilibrium shift takes place in the supercooled and the glassy solutions:

$$2\,[ZnX_2(OH_2)_2] + 2\,H_2O \rightarrow [ZnX_4]^{2-} + [Zn(OH_2)_6]^{2+} \quad (X^- = Br, I), \quad (1)$$

$$4\,[ZnX_3(OH_2)]^- + 2\,H_2O \rightarrow 3\,[ZnX_4]^{2-} + [Zn(OH_2)_6]^{2+} \quad (X^- = Br). \quad (2)$$

The two equilibrium shifts to the right-hand-side with decreasing temperature have been explained by strengthened hydrogen bonding of the water-water and the anion-water interactions.

For temperatures up to 300 °C and pressures up to 9 MPa, Yang et al. [25] have recorded Raman spectra for a 3.72 m aqueous zinc(II) bromide solution and have suggested that the amount of the dibromozinc(II) complex increases with rising temperature, whereas that of the tetrabromo species decreases.

In the present study we have performed combined Raman and X-ray scattering measurements on a zinc(II) bromide solution with molar ratio $[H_2O]/[ZnBr_2] = 10$ from ambient temperature to 140 °C, and in combination with our result from [24] we discuss the shift of the chemical equilibrium with temperature in the range from liquid nitrogen temperature to 140 °C on the basis of the ion-ion, ion-water, and water-water interactions.

	Sample
Zn^{2+}	5.493
Br^-	10.99
ϱ	1.761
V	3.841
$[H_2O]/[ZnBr_2]$	10.11

Table 1. Concentrations (mol/kg H_2O), density ϱ (g cm^{-3}) at 25 °C, the stoichiometric volume V (10^8 pm^3) per Zn atom and water/salt molar ratio.

2. Experimental

2.1. Preparation of Sample Solutions

Zinc(II) bromide (Wako Pure Chemicals, 99.9%) was used without further purification and dissolved in distilled water to reach the $[H_2O]/[ZnBr_2]$ molar ratio 10. The concentration of zinc(II) ions in a sample solution was determined by titration of an EDTA standard solution using Eriochrome Black T as an indicator. The density of the sample solution at 25 °C was measured pycnometrically, and those above 25 °C were estimated from the densities in the temperature range 5 to 100 °C given in [26]. The composition and density data at 25 °C of the sample solution are given in Table 1.

2.2. Raman Spectral Measurements

The sample solution was sealed in glass capillary tubes of 1.8 mm inner diameter. A JEOL JRS-400T spectrometer was used to record Raman spectra at 25, 40, 60, 80, 100, 120, and 140 °C. The temperatures were measured with a copper-constantan thermocouple and controlled within ±1 °C by hot air and cooling water. The 514.5 nm line radiated from an argon ion laser (Spectra Physics, Model 168 B) was used for all measurements.

2.3. X-ray Diffraction Measurements and Data Treatment

X-ray diffraction measurements were performed at 25, 40, 80, and 100 °C using a Rigaku $\theta-\theta$ type diffractometer. An X-ray tube was used to irradiate MoKα radiation ($\lambda = 71.07$ pm). X-rays scattered from the free surface of the sample solution were monochromatized with a LiF (200) bend crystal. The observed range of the scattering angle (2θ) was from 2° to 140°, corresponding to the scattering vector s ($= 4\pi \sin\theta/\lambda$) of 3.1×10^{-3} to 0.166 pm^{-1}. The measurements were repeated twice over the whole angle range. Different slit combinations and step angles were used depending on the angle range, and a total amount of 20 000 counts was collected at each angle. The details of the X-ray diffraction measurements have been described

in [27, 28]. The temperature of the sample was measured with a copper-constantan thermocouple and controlled within ± 0.2 °C by use of a temperature control system with a heating unit described in [23].

The measured intensities of X-rays, $I(s)$, were corrected in the usual way [29] for background, absorption, and polarization of the X-rays. The corrected intensities were then normalized to electron units by the conventional methods [30–32]. The contribution of the incoherent scatterings, $\sum x_i \phi(s) I_i^{\text{inco}}(s)$, was deduced from the normalized intensities, where x_i is the number of atom i in a stoichiometric volume V containing one Zn atom, $\phi(s)$ the fraction of the incoherent radiation, $I_i^{\text{inco}}(s)$, reaching a scintillation counter. Correction only for the double scattering was made by the method described in [33]. The structure function, $i(s)$, is given by

$$i(s) = I^{\text{coh}}(s) - \sum_i x_i f_i^2(s), \tag{3}$$

where $f_i(s)$ represents the atomic scattering factor of atom i corrected for the anomalous dispersion.

The s-weighted structure function is Fourier transformed into the radial distribution function $D(r)$ as

$$D(r) = 4\pi r^2 \varrho_0 + \frac{2r}{\pi} \int_0^{s_{\max}} s\, i(s)\, M(s) \sin(rs)\, \mathrm{d}s. \tag{4}$$

Here, $\varrho_0 (= [\sum n_i f_i(0)]^2 / V)$ stands for the average scattering density of a sample solution, $s_{\max}$ is the maximum s-value attained in the measurements ($s_{\max} = 0.166\ \text{pm}^{-1}$). A modification function $M(s)$ of the form $[\sum x_i f_i^2(0) / \sum x_i f_i^2(s)] \exp(-100 s^2)$ was used for the sample solution.

A comparison between the experimental structure function and the theoretical one based on a model was made by a least-squares refinement procedure of minimizing the error square sum,

$$U = \sum_{s_{\min}}^{s_{\max}} s^2 \{i(s)_{\text{exp}} - i(s)_{\text{calc}}\}^2. \tag{5}$$

The theoretical intensities $i(s)_{\text{calc}}$ were calculated by

$$i(s)_{\text{calc}} = \sum_i \sum_{j \neq i} x_i n_{ij} f_i(s) f_j(s) \frac{\sin(r_{ij} s)}{r_{ij} s} \exp(-b_{ij} s^2) - \sum_i \sum_{j \neq i} x_i x_j f_i(s) f_j(s) \frac{4\pi R_j^3}{V} \frac{\sin(R_j s) - R_j s \cos(R_j s)}{(R_j s)^3} \cdot \exp(-B_j s^2). \tag{6}$$

The first term of the right-hand-side of (6) is related to the short-range interactions characterized by the interatomic distance r_{ij}, the temperature factor b_{ij}, and the number of interactions n_{ij} for atom pair $i-j$. The second term arises from the interaction between a spherical hole and the continuum electron distribution beyond this discrete distance. R_i is the radius of the spherical hole around the i-th atom and B_i the softness parameter for emergence of the continuum electron distribution.

All treatments of the X-ray diffraction data were carried out with programs KURVLR [29] and NLPLSQ [34].

3. Results and Discussion

3.1. Raman Spectra

Raman spectra for the aqueous zinc(II) bromide solution at various temperatures are shown in Figure 1. In the Raman spectrum at 25 °C three Raman bands are observed at 207, 185, and 171 cm^{-1}, which are attributed to the ν_1 mode of the totally symmetric Zn–Br stretching vibration within the dibromo-, the tribromo-, and the tetrabromozinc(II) complexes, respectively, according to studies by Kanno and Hi-

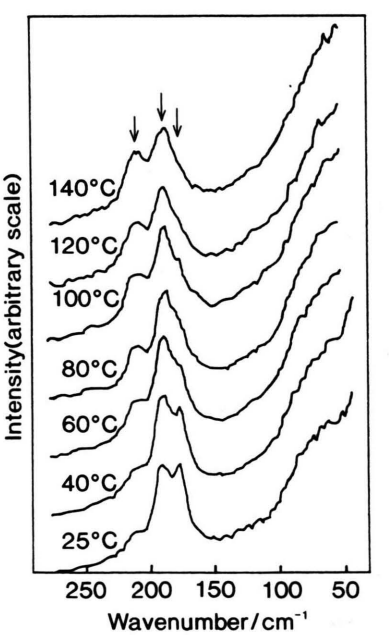

Fig. 1. Raman spectra for the studied aqueous zinc(II) bromide solution at various temperatures.

raishi [22] and by Yang et al. [25]. As seen in Fig. 1, the intensity of the ν_1 mode (207 cm^{-1}) for the dibromozinc(II) complex increases gradually with rising temperature, whereas that (171 cm^{-1}) for the tetrabromozinc(II) complex decreases with temperature. The intensity of the band (185 cm^{-1}) for the tribromozinc(II) complex changes little with temperature. Similar intensity changes of the Raman bands with temperature have been observed for a 3.72 m aqueous zinc(II) bromide solution at temperatures ranging from 25 to 300 °C by Yang et al. [25]. These Raman bands, however, do not shift significantly with temperature.

Yang et al. [25] have found a new Raman band at 240 cm^{-1}, related to the monobromo species, for a less concentrated (3.72 m) $ZnBr_2$ aqueous solution at temperatures above 200 °C; the intensity of this band increases with rising temperature. As seen in Fig. 1 the corresponding band for the monobromo species is not observed even at 140 °C; this suggests that the monobromozinc(II) complex is not formed to an appreciable amount in the present solution.

A broad Raman spectrum around 390 cm^{-1} at the various temperatures is shown in Figure 2. According to a Raman spectroscopic study for a 3.36 m aqueous zinc(II) nitrate solution by Bulmer et al. [1], this band is assignable to the ν_1 mode of the totally symmetric Zn–O stretching vibration within the aqua zinc(II) ion. As seen in Fig. 2, the intensity of this band decreases with increasing temperature, suggesting that the formation of this aqua zinc(II) species is less favored at elevated temperatures.

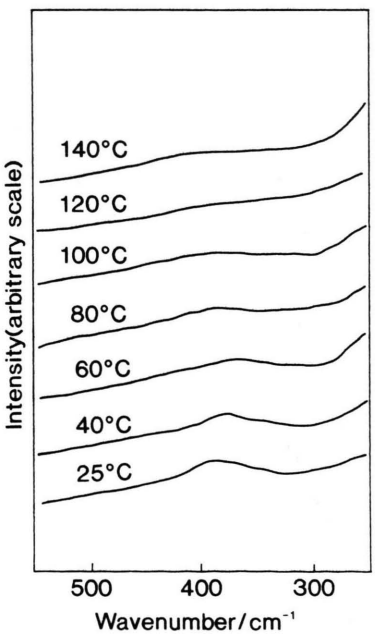

Fig. 2. Raman spectra for the studied aqueous zinc(II) bromide solution at various temperatures.

The tendency of the ν_1 bands due to the Zn–Br and Zn–O vibrations observed at temperatures above 25 °C is consistent with that found in the supercooled and glassy solutions [24]. From both present and previous [24] Raman spectroscopic studies on the aqueous zinc(II) bromide solution, therefore, it is concluded that the composition of zinc(II) bromo complexes present in the zinc(II) bromide solution changes successively with temperature; the tetrabromo and the aqua zinc(II) complexes are formed preferably in the supercooled and glassy aqueous solutions, whereas the amount of the dibromo complex in the solution increases with rising temperature.

3.2. X-ray Scattering

The structure functions weighted with s for the sample solution at various temperatures are shown in Figure 3. The corresponding total radial distribution functions (RDFs), $D(r)-4\pi r^2\varrho_0$, are depicted in Figure 4. Three large peaks appear at 239, 390, and 550–850 pm in the total RDFs at all temperatures. The first sharp peak arises mainly from the Zn–Br interactions within the zinc(II) bromo complexes formed in the solution. This peak is expected to include a peak due to the Zn–O interactions within the aqua zinc(II) species, which should appear around 210 pm [13–16]. The second peak is assigned mainly to the nonbonding Br ··· Br interactions within the various tetrahedral zinc(II) bromo complexes, since the ratio (~1.66) of the Br ··· Br to the Zn–Br distances is close to the expected value ($[8/3]^{1/2}=1.63$). Furthermore, the second peak has a shoulder at about 360 pm, which is due to the nonbonding Br ··· H_2O interactions within the dibromo- and tribromozinc(II) complexes, $[ZnBr_2(OH_2)_2]$ and $[ZnBr_3(OH_2)]^-$, respectively. According to an X-ray diffraction study on a single crystal of $KZnBr_3 \cdot H_2O$ [35], various interactions between a central zinc(II) ion and atoms in the second coordination shell and between atoms in the first and the second shells contribute to the total RDF in the range of 335–490 pm. The interactions between water molecules in the first and the second coordination shells, H_2O ··· H_2O, were taken into account for

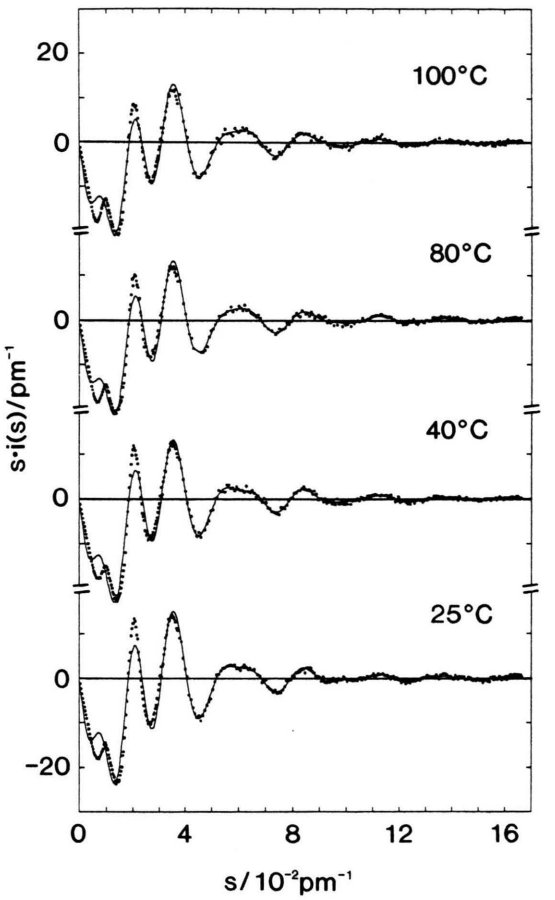

Fig. 3. Structure functions $i(s)$ multiplied by s for the zinc(II) bromide solution at various temperatures. The experimental values are drawn by dots, and those calculated with the parameter values given in Tables 2 and 3 by solid lines.

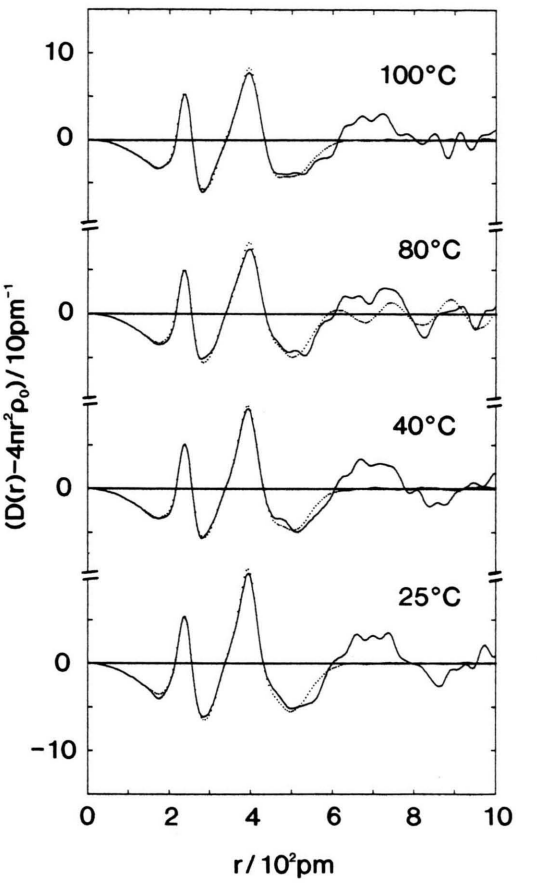

Fig. 4. Radial distribution functions in the form of $D(r)-4\pi r^2\varrho_0$ for the zinc(II) bromide solution at various temperatures: experimental (solid lines) and calculated (dotted lines), which are obtained by Fourier transform of the values in Figure 3.

the sample solution above 40 °C, since the lower complex, $[ZnBr_2(OH_2)_2]$, becomes dominant in the solution. The broad peak at 550–850 pm, which should originate from long-range intermolecular interactions, was not analyzed in the present study; instead, an even electron distribution was assumed. As seen in Fig. 4, the first peak does not change significantly with temperature, but the intensity of the second peak decreases gradually with the increase in temperature. Furthermore, the shoulder at about 360 pm is enhanced at higher temperatures.

A least-squares fitting procedure was applied to the structure functions over the range of $0.1\times10^{-2}< s/\mathrm{pm}^{-1}<0.166$ in order to characterize the structure parameters for the sample solution. In the present calculation, the interatomic distance r, the temperature factor b, the number of interactions n, and parameters R and B for a continuum electron distribution were refined; the optimized values are summarized in Tables 2 and 3. For comparison, the values previously obtained for a supercooled aqueous zinc(II) bromide solution with molar ratio $[H_2O]/[ZnBr_2]=5$ at −40 °C [24] are also listed in Tables 2 and 3. The theoretical $si(s)$ and RDFs calculated by using the optimized values in Tables 2 and 3 reproduced well the observed ones except the range of the long-range interactions not taken into account, as seen in Figs. 3 and 4.

In Table 2 the number of Zn–Br interactions changes little with temperature, $n(\mathrm{Zn-Br})\approx2$, but the number of nonbonding Br ··· Br interactions decreases from 1.81(7) at 25 °C to 1.54(8) at 100 °C. The

Table 2. Optimized parameter values of the interactions within the zinc(II) bromide complexes for the sample solution at various temperatures: the interatomic distance r (pm), the temperature factor b (pm^2), the number of interactions n per zinc(II) ion. The values in parentheses are their standard deviations estimated from the least-squares refinements. The parameters without standard deviations were fixed during the calculations. – [a] Ref. [24].

Interaction	Parameter	−40 °C [a]	25 °C	40 °C	80 °C	100 °C
Zn–O	r	210	207	201	203	202
	$b/10$	5	5	5	5	5
	n	3.0	2.7	2.1	2.0	2.0
Zn–Br	r	239.4(2)	238.6(3)	238.6(3)	237.6(3)	237.3(3)
	$b/10$	2	5	5	5	5
	n	2.03(2)	2.00(3)	1.98(3)	1.94(3)	1.99(3)
Br ··· Br	r	390.3(4)	393.7(7)	392.8(7)	397.2(8)	397.3(10)
	$b/10$	20	20	20	20	20
	n	2.41(5)	1.81(7)	1.78(7)	1.69(8)	1.54(8)
Br ··· H_2O	r	360	360	360	360	360
	$b/10$	10	20	20	20	20
	n	0.7	2.0	2.3	2.7	2.8

Table 3. Optimized parameter values of the medium-range interactions and of the continuum electron distribution for the sample solution at various temperatures: the interatomic distance r (pm), the temperature factor b (pm^2), the number of interactions n per zinc(II) ion, and parameters for continuum electron distribution R (pm) and B (pm^2). The values in parentheses are their standard deviations estimated from the least-squares refinements. The parameters without standard deviations were fixed during the calculations. – [a] Ref. [24].

Interaction	Parameter	−40 °C [a]	25 °C	40 °C	80 °C	100 °C
H_2O ··· H_2O	r	–	–	280	280	280
	$b/10$	–	–	20	20	20
	n	–	–	6.0	6.5	6.5
Zn ··· H_2O	r	396	395	395	395	395
	$b/10$	10	10	15	20	15
	n	11.8	9.0	8.5	7.0	7.5
Br ··· H_2O	r	333	338	334	337	337
	$b/10$	10	15	20	20	20
	n	5.0	6.0	6.5	5.5	6.5
Zn ··· H_2O	r	494	474	479	470	484
	$b/10$	10	10	10	10	10
	n	0.6	1.5	2.7	2.2	2.2
Br ··· H_2O	r	458	448	440	435	434
	$b/10$	20	15	15	20	20
	n	7.0	3.0	2.8	2.8	2.8
Zn	R	258(7)	255(18)	262(12)	273(18)	277(13)
	$B/10$	10	10	10	10	10
Br	R	515(2)	517(2)	516(2)	511(2)	513(2)
	$B/10$	65(12)	98(16)	90(15)	85(14)	105(16)
H_2O	R	355(3)	326(3)	346(2)	338(3)	352(2)
	$B/10$	10	127(47)	103(32)	105(44)	102(37)

decrease in n(Br–Br) of 0.27 is beyond estimated uncertainties in the present X-ray analysis. This behavior of n suggests that the tetrabromo and the aqua zinc(II) complexes become less favored, but the lower zinc(II) bromo complexes such as the dibromo species are predominantly formed with increasing temperature; this result is consistent with that deduced from the Raman spectra described in the previous section.

The Zn–Br distance for the zinc(II) bromo complexes in the solution decreases slightly from 238.6(3) pm at 25 °C to 237.3(3) pm at 100 °C. The increase in the distance of Br ··· Br nonbonding interactions is more significant; 393.7(7) pm at 25 °C to 397.3(10) pm at 100 °C. According to the previous study for the supercooled aqueous zinc(II) bromide solution [24], in which the fraction of the tetrabromo species in-

creases with lowering temperature, both distances for the Zn–Br and the Br···Br interactions do not change within experimental uncertainties in the temperature range between −5 and −40 °C and are 239.4(2) and 390.3(4) pm, respectively, as given in Table 2. By using the values of the Zn–Br and Br–Br distances, an average Br–Zn–Br bond angle within the zinc(II) bromo complexes is calculated to be 109° at −40 °C and 114° at 100 °C; this result indicates that the tetrahedral moiety is more distorted for the dibromo complex than for the tetrabromo species. Goggin et al. [15] have determined the structure of the individual zinc(II) bromo complexes in aqueous solution at ambient temperature with X-ray diffraction; the Zn–Br and Br–Br distances, and the Br–Zn–Br angle for the tetrabromo complex are 240.8 pm, 393 pm, and 109°, respectively, and those for the dibromo species are 238.6 pm, 401 pm, and 114°, respectively. These values are in good agreement with the present finding, which again confirms that the predominant species in the solution at 100 °C is the dibromo complex whereas in the supercooled solution at −40 °C the tetrahedral tetrabromo species is mainly formed. These X-ray results are consistent with the conclusion from the Raman spectral measurements.

3.3. Equilibrium Shifts with Temperature

Both the present and the previous [24] studies suggest that the following equilibrium shifts occur in the zinc(II) bromide solution when the temperature is lowered:

$$3\,[ZnBr_2(OH_2)_2] + 2\,H_2O \rightarrow 2\,[ZnBr_3(OH_2)]^- + [Zn(OH_2)_6]^{2+}, \quad (7)$$

$$4\,[ZnBr_3(OH_2)]^- + 2\,H_2O \rightarrow 3\,[ZnBr_4]^{2-} + [Zn(OH_2)_6]^{2+}. \quad (8)$$

The above equilibria may be discussed on the basis of thermodynamic data on the zinc(II)-bromide system in aqueous solution. Only a few thermodynamic studies [11, 12] have so far been made on the complex formation of the zinc(II)-bromide system in aqueous solution at ambient temperature because the complex formation between zinc(II) and bromide ions is relatively weak in aqueous solution. Shchukarev et al. [11] have determined the stepwise enthalpy from the stability constants measured at different temperatures. The values for ΔH_n^0 are 0, 0, 26.4, and −28.4 kcal mol^{-1} for $n=1, 2, 3$, and 4, respectively [11]. Only the fourth step takes place exothermally, whereas the other steps occur endothermally in an aqueous zinc(II) bromide solution. If this tendency did not change significantly over the temperature range used in the present system, it would be expected that the lower complexes are favored at the higher temperatures, whereas the tetrabromo complex is formed preferentially with lowering temperature. This expectation holds good in the present solution as demonstrated by the present and the previous [24] results from the Raman and X-ray measurements.

We now discuss the equilibrium shifts (7) and (8) from a microstructural point of view. The complex formation between zinc(II) and bromide ions in aqueous solution is affected by the ion-ion, ion-water, and water-water interactions. The magnitude of the interaction between zinc(II) and bromide ions will not change appreciably with temperature. In fact the ν_1 band, due to a totally symmetric Zn–Br vibration within the individual zinc(II) bromo complex, does not shift significantly with temperature, as seen in the Raman spectra (Fig. 1 and [24]). However the strength of the ion-water and water-water interactions will greatly depend on the temperature.

At temperatures below the melting point of water, the hydrogen bonds between nearest-neighbor water molecules and between bromide ion and water molecules are strengthened as has been discussed in previous papers [23, 24, 36]. Hence, water molecules dispelled from the coordination shells of the dibromo- and tribromo complexes are stabilized in the strengthened hydrogen-bond network; thus the bromide ion will more easily bind to a zinc(II) ion to form the tetrabromo complex. On the contrary, the hydrogen-bond network will be gradually broken from ~75% at 25 °C to ~40% at 180 °C, as revealed by X-ray [37] and neutron [38, 39] diffraction investigations on liquid water at 25–200 °C. In the present zinc(II) bromide solution at the high temperatures, therefore, a large amount of water molecules not involved in the hydrogen bonding will be able to bind to zinc(II) ions more frequently than bromide ions, since water is 5 times more concentrated than bromide ion in the solution. Consequently, the dibromozinc(II) complex is in the present solution formed preferentially at high temperatures. The monobromo complex, $[ZnBr(OH_2)_5]^+$ [15], would be formed in less concentrated $ZnBr_2$ aqueous solution at much higher tem-

peratures, as observed for a 3.72 m aqueous zinc(II) bromide solution at temperatures above 200 °C by Yang et al. [25]. In the present solution, however, the monobromo species is not formed significantly even at 140 °C, probably because the water content in the solution is too low to form the monobromo species and hydrated bromide ion.

4. Concluding Remarks

From the combination of the present and previous [24] studies of a concentrated aqueous zinc(II) bromide solution with the molar ratio $[H_2O]/[ZnBr_2] = 10$ it is concluded that the dibromozinc(II) complex is favored at high temperature, while the amount of tetrabromo and aqua zinc(II) complexes increases gradually with lowering temperature. Water does play an important role in the equilibrium shifts (7) and (8), since the water-water interaction is affected more drastically by temperature than the affinity between the metal and ligand ions. These temperature dependent interactions are a key to understand the variation of chemical equilibrium and physico-chemical data with temperature.

Acknowledgements

The present work was partially supported by a Grant-in-Aid for Scientific Research in the Priority Area of "Molecular Approaches to Non-equilibrium Processes in Solutions" (No. 03231105) from the Ministry of Education, Science and Culture, Japan. All the calculations were performed at the Computer Center of Fukuoka University.

[1] J. T. Bulmer, D. E. Irish, and L. Ödberg, Can. J. Chem. **53,** 3806 (1975).
[2] B. G. Anderson and D. E. Irish, J. Solution Chem. **17,** 763 (1988).
[3] K. Murata, D. E. Irish, and G. E. Toogood, Can. J. Chem. **67,** 517 (1989).
[4] G. W. Neilson, Chem. Phys. Lett. **68,** 247 (1979).
[5] G. W. Neilson and S. Cummings, Rev. Phys. Appl. **19,** 803 (1984).
[6] A. Y. Wu, E. Whalley, and G. Dolling, Mol. Phys. **47,** 603 (1982).
[7] M. A. Bernhard, F. Busnot, and J. F. Le Querler, Bull. Soc. Chim. Fr. **1972,** 4523.
[8] R. F. Kruh and C. L. Standley, Inorg. Chem. **1,** 941 (1962).
[9] Y. Nakamura, S. Shimokawa, K. Futamata, and M. Shimoji, J. Chem. Phys. **77,** 3258 (1982).
[10] S. Ahrland, L. Kullberg, and R. Portanova, Acta Chem. Scand. **A 32,** 251 (1978).
[11] S. A. Shchukarev, L. S. Lilich, and V. A. Latysheva, Zh. Neorg. Khim. **1,** 225 (1956).
[12] P. Gerding, Acta Chem. Scand. **23,** 1695 (1969).
[13] (a) D. L. Wertz and J. R. Bell, J. Inorg. Nucl. Chem. **35,** 137 (1973). (b) ibid. **35,** 861 (1973).
[14] T. Yamaguchi, S. Hayashi, and H. Ohtaki, J. Phys. Chem. **93,** 2620 (1989).
[15] P. L. Goggin, G. Johansson, M. Maeda, and H. Wakita, Acta Chem. Scand. **A 38,** 625 (1984).
[16] H. Wakita, G. Johansson, M. Sandström, P. L. Goggin, and H. Ohtaki, J. Solution Chem. **20,** 643 (1991).
[17] D. E. Irish, Ionic Interactions, Vol. II (S. Petrucci, ed.), Academic Press, New York 1971, pp. 239–246.
[18] (a) M. L. Delwaulle, C. R. Acad. Sci. Paris **240,** 2132 (1955). (b) M. L. Delwaulle, Bull. Soc. Chim. Fr. **1955,** 1294.
[19] D. E. Irish, B. M. McCarroll, and T. F. Young, J. Chem. Phys. **39,** 3426 (1963).
[20] D. F. C. Morris, E. L. Short, and K. Slater, Electrochim. Acta **8,** 289 (1963).
[21] M. P. Fontana, G. Maisano, P. Migliardo, and F. Wanderlingh, J. Chem. Phys. **69,** 676 (1978).
[22] H. Kanno and J. Hiraishi, J. Raman Spectrosc. **9,** 85 (1980).
[23] T. Takamuku, T. Yamaguchi, and H. Wakita, J. Phys. Chem. **95,** 10098 (1991).
[24] T. Takamuku, K. Yoshikai, T. Yamaguchi, and H. Wakita, submitted for publication.
[25] M. M. Yang, D. A. Crerar, and D. E. Irish, J. Solution Chem. **17,** 751 (1988).
[26] O. Söhnel and P. Novotný, ed., Physical Sciences Data 22, Densities of Aqueous Solutions of Inorganic Substances, Elsevier, New York 1985.
[27] H. Wakita, M. Ichihashi, T. Mibuchi, and I. Masuda, Bull. Chem. Soc. Japan **55,** 817 (1982).
[28] T. Yamaguchi, G. Johansson, B. Holmgerg, M. Maeda, and H. Ohtaki, Acta Chem. Scand. **A 38,** 437 (1984).
[29] G. Johansson and M. Sandström, Chem. Scr. **4,** 195 (1973).
[30] K. Furukawa, Rep. Progr. Phys. **25,** 395 (1962).
[31] J. Krogh-Moe, Acta Crystallogr. **2,** 951 (1956).
[32] N. Norman, Acta Crystallogr. **10,** 370 (1957).
[33] B. E. Warren and R. L. Mozzi, Acta Crystallogr. **21,** 459 (1966).
[34] T. Yamaguchi, Doctoral Thesis, Tokyo Institute of Technology, 1978.
[35] Von R. Holinski and B. Brehler, Acta Crystallogr. **B 26,** 1915 (1970).
[36] H. Kanno and J. Hiraishi, J. Phys. Chem. **87,** 3664 (1983).
[37] A. H. Narten and H. A. Levy, J. Chem. Phys. **55,** 2263 (1971).
[38] T. Yamaguchi, Y. Tamura, H. Ohtaki, S. Ikeda, and M. Misawa, KENS Report, National Laboratory for High Energy Physics, Oho, Tsukuba, Japan **6,** 125 (1986).
[39] A. K. Soper and T. Yamaguchi, ISIS Annual Report, Rutherford Appleton Laboratory, Chilton, Didcot, Oxon, OX11 0QX, U.K., A110 (1991).